

## A CALCULUS FOR BRANCHED SPINES OF 3-MANIFOLDS

FRANCESCO COSTANTINO

Abstract. We establish a calculus for branched spines of 3-manifolds by means of branched Matveev-Piergallini moves and branched bubble moves. We briefly indicate some of its possible applications in the study and definition of State-Sum Quantum Invariants.

## Contents

1. Introduction	1
2. Preliminaries	2
3. A calculus for branched spines of 3-manifolds	7
References	15

## 1. Introduction

Since the establishment of Matveev-Piergallini calculus, simple spines of 3-manifolds have been one of the most powerful tools to study these spaces. They allowed a combinatorial approach to many fundamental topics as the study of State-Sum Quantum Invariants and the study of complexity of 3-manifolds.

Branched spines of 3-manifolds, which could be viewed as the smoothed version of simple spines, were first introduced and studied by Benedetti and Petronio in [5]. Among other substantial results, in this book, Benedetti and Petronio showed that each 3-manifold has a branched spine and identified the topological structure encoded by these objects on the ambient manifolds as a particular class of non-singular vector fields they called Concave Transversing Fields. At a more rough level, it can be showed that branched spines can be used to represent the  $\text{Spin}^c$ -structures on the ambient manifolds.

In the present work, instead of viewing branched spines as a tool to represent 3-manifolds equipped with additional structures, we will use these objects to re-obtain a representation theory of naked 3-manifolds. To clarify the reason why we are interested in such a representation theory we notice that a branched spine is much less symmetric than a non-branched one. Moreover, a branched spine is dual to a triangulation of the ambient manifold whose "abstract" tetrahedra can be canonically "parametrized" by the standard simplex  $(v_0; v_1; v_2; v_3)$  in  $\mathbb{R}^3$ : indeed, using the branching, we can canonically identify in each dual tetrahedron the vertex corresponding to each  $v_i$ ,  $i = 0; \dots; 3$ .

This kind of branched triangulations underlie the definition of the Quantum Invariants obtained as State-Sum and this is their main motivation for the present note. Indeed, using these objects, S. Basile and R. Benedetti constructed in [2] and [3] (see also [1]) the so-called classical and quantum dilogarithmic invariants for 3-manifolds equipped with principal  $\text{PSL}(2; \mathbb{C})$ -bundles.

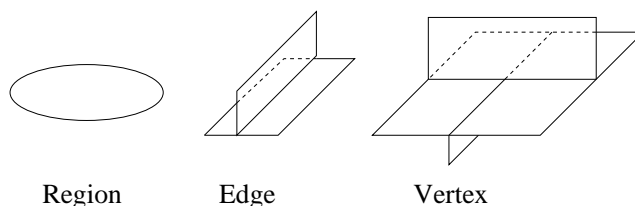


Figure 1. The local models of a simple polyhedron.

In the present paper we show, in particular, that two branchings on a given triangulation can be connected by means of a finite sequence of basic (2 ! 3, and "bubble") branched modification of branched triangulations. With the terminology of Baseilhac-Benedetti, this implies that the branching state sum invariance is a consequence of its transit invariance.

Before plunging into the details, let us note that what we call "calculus for branched spines" should be better called "calculus for branched skeleta" in the sense that we show that two branched spines of the same 3-manifold are connected by a sequence of moves which contains an (algebraic) number of bubble-moves equal to zero; hence, during the sequence, the spines could be transformed into spines of the manifold obtained by puncturing the ambient manifold, which are also called skeleta of the initial manifold. Fortunately this causes no harm since the initial ambient manifold can always be canonically reconstructed from a skeleton. In terms of dual triangulations this means the natural fact that the number of vertices is not fixed.

Acknowledgements. The author wishes to warmly thank Riccardo Benedetti and Stephane Baseilhac for their encouraging comments and illuminating critics.

## 2. Preliminaries

In this section we recall the notion of branched polyhedron and some basic facts about branched spines of 3-manifolds. From now on, we will deal only with polyhedra which have the property of containing only regions which are orientable surfaces (this is due to our definition of branching, see Definition 2.2) and with oriented 3-manifolds.

A simple polyhedron is a finite polyhedron of dimension 2 whose local models are the three shown in Figure 1. An embedded spine of a 3-manifold  $M$  is a simple polyhedron  $P$  embedded in  $M$  in a locally flat way (i.e. so that there exist local charts as those shown in Figure 1) so that  $M$  retracts on  $P$  (if  $\partial M \neq \emptyset$ ) or  $M$  (if  $\partial M = \emptyset$ ) retracts on  $P$  (if  $\partial M = \emptyset$ ).

The singular set of a simple polyhedron  $P$ , denoted by  $\text{Sing}(P)$ , is the union of the edges and vertices (see Figure 1). The regions of a simple polyhedron  $P$  are the connected components of the complement of a small open regular neighborhood of  $\text{Sing}(P)$ .

A simple polyhedron is said to be standard if its regions are all discs, its singular set is connected and contains at least a vertex. It is well known that any 3-manifold admits a spine, even a standard one, moreover the following holds:

**Theorem 2.1 (Matveev-Piergallini).** Any two standard spines of the same 3-manifold are connected by means of a suitable sequence of local moves (and their inverses) as the one shown in the lower part of Figure 2 and called the 2 ! 3-move. More in general, two simple spines of the same 3-manifold are connected by a suitable sequence of this move and moves of the type shown in the upper part of Figure 2 and their inverses; this last move is called the line-move or 0 ! 2-move.

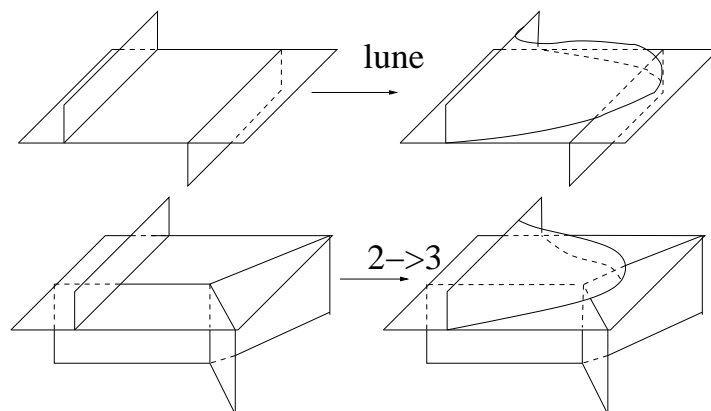


Figure 2. In this figure we show the basic moves for polyhedra. Note that both moves create a new region: the small disc entirely contained in the left part of the figures.

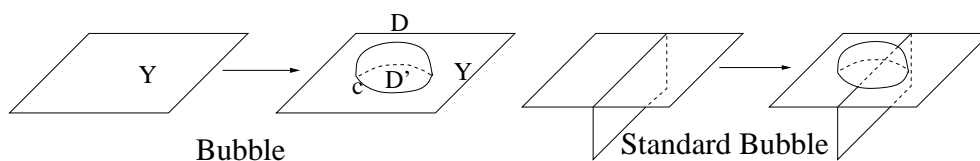


Figure 3. In the left part of the figure we show the bubble move; it can be interpreted as the gluing of a disc  $D$  along its boundary to a simple closed curve  $c$  contained in the interior of a region  $Y$  and bounding a small disc  $D^0$ . The result of the application of such a move to a standard polyhedron is not a standard polyhedron, so often one uses its standard version, shown in the right part of the picture.

The above Theorem is the well known Calculus for spines of 3-manifolds proved independently by Matveev and Piergallini respectively in [9] and [11].

Another local move we will use is called bubble move it is applied in the interior of a region and its effect is drawn in Figure 3.

Given a simple polyhedron  $P$  we define the notion of branching on it as follows:

**Definition 2.2 (Branching condition).** A branching  $b$  on  $P$  is a choice of an orientation of each region of  $P$  such that no edge of the singular set of  $P$  is induced three times the same orientation by the regions containing it.

**Remark 2.3.** This definition corresponds to the definition of "orientable branching" given in [5].

Not all the simple polyhedra admit a branching and, on the contrary, there are some which admit more than one (see [5], Chapter III). We will say that a polyhedron is branchable if it admits a branching and we will call branched polyhedron a pair  $(P; b)$  where  $b$  is a branching on the polyhedron  $P$ .

**Definition 2.4.** Let  $P$  be a spine of an oriented 3-manifold  $M$ ;  $P$  is said to be branchable if the underlying polyhedron is. We call branched spine of  $M$  the pair  $(P; b)$  where  $P$  is a

spine and  $b$  is a branching on the underlying polyhedron. When this will not cause any confusion, we will not specify the branching  $b$  and we will simply write  $P$ .

A branching on a simple polyhedron allows us to smoothen its singularities and equip it with a smooth structure as shown in Figure 4.

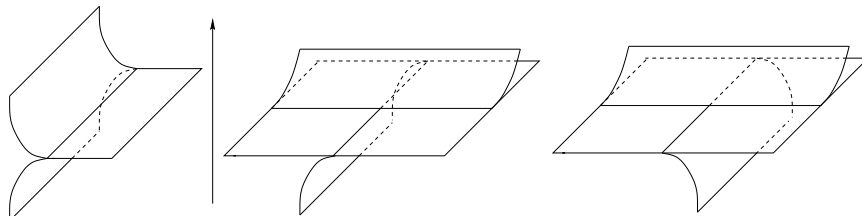


Figure 4. How a branching allows a smoothing of the polyhedron: the regions are oriented using the right-hand rule, the upward direction and the orientation of the ambient 3-manifold (coinciding with the standard one of the chart depicted here).

If  $P$  is a branched spine of a 3-manifold, and we apply to it a basic move (one of the moves of Figure 2), we get another spine  $P^0$  of the same manifold containing one region more than  $P$ . Moreover, each region of  $P$  naturally corresponds to a region of  $P^0$  and the region of  $P^0$  which does not correspond to one of  $P$  is the small disc created by the move (see Figure 2). Hence the branching on  $P$  induces a choice of an orientation on each region of  $P^0$  except on that disc and these orientations satisfy the branching condition on all the edges of  $P^0$  not touched by that disc. Analogously, if  $P^0$  is obtained from  $P$  through the inverse of a basic move, then each region of  $P^0$  corresponds to a region of  $P$  and hence the branching on  $P$  induces an orientation on each region of  $P^0$ .

**Definition 2.5.** A basic move  $P \rightarrow P^0$  applied on a branched polyhedron  $P$  is called *branchable* if it is possible to choose an orientation on the disc created by the move which, together with the orientations on the regions of  $P^0$  induced by the branching of  $P$ , defines a branching on  $P^0$ . Analogously, the inverse of a basic move applied to  $P$  is *branchable* if the orientations induced by the branching of  $P$  on the regions of  $P^0$  define a branching.

A branching is a kind of loss of symmetry on a polyhedron and this is reflected by the fact that each move has many different branched versions. To enumerate all the possible embedded branched versions of the moves, one has to fix any possible orientation on the regions of the left part of Figure 2 and then complete these orientations in the right part of the figure by fixing one orientation on the region created by the move; by Definition 2.5, one obtains a branched version of a basic move when the branching condition is satisfied both in the left and in the right part of the figure. Fortunately, many of the possible combinations are equivalent up to symmetries of the pictures, so that all the resulting local moves have been classified in [5]. We show them in Figure 5 for the lune-move and in Figure 6 for the  $2 \rightarrow 3$ -move. In these figures we split these branched versions in two types namely the sliding-moves and the bumping-moves; this differentiation will be used when stating Theorem 2.6.

We note here that in some cases both orientations on the region created by a move satisfy the branching condition, and this produces different branched versions of the same move. This is the case of the bumping moves: for instance in the lower part of Figure 6 the orientation fixed on the disc created by the move is such that the leftmost region and

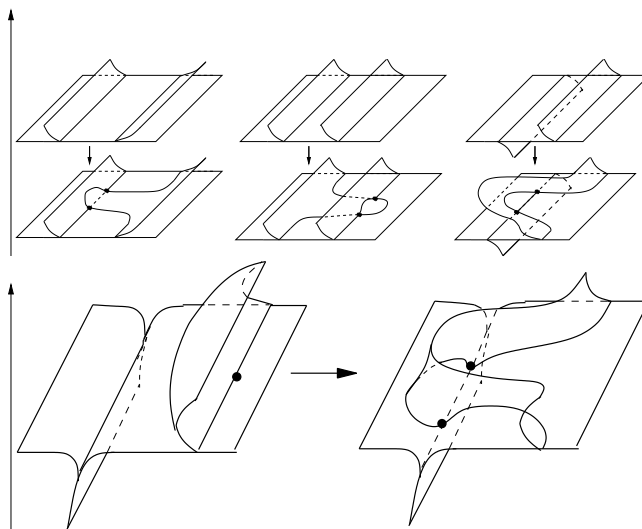


Figure 5. In the upper part of this figure we show the three branched versions of the lune move called "sliding" moves. In the bottom part we show the version called "bumping" move. The arrow on the left indicates the vertical direction.

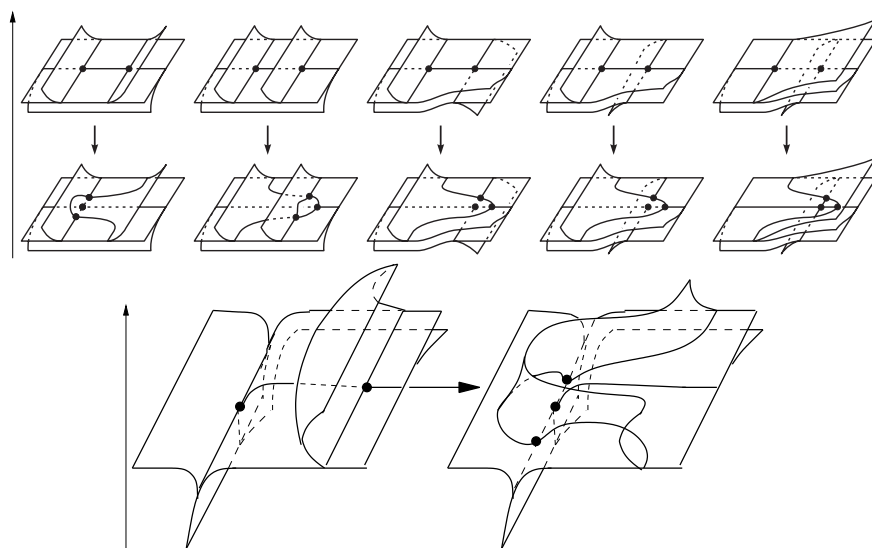


Figure 6. In the upper part of the figure we show the 5 branched versions of the  $2!3$  move called "sliding" moves. In the bottom part of the figure we show the version called "bumping" move. The arrow on the left indicates the vertical direction.

the disc induce opposite orientations on the edge separating them, so that the disc appears as a smooth continuation of the leftmost region out of that edge. The same phenomenon happens for leftmost sliding moves in Figures 5 and 6. In these cases, exploiting the

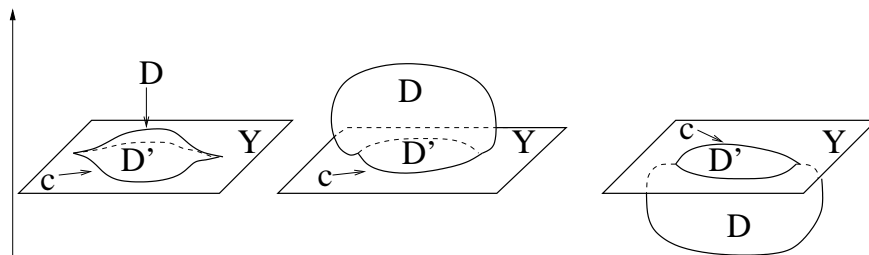


Figure 7. In this figure we draw the 3-versions of the embedded branched bubble move: the left-most one is called "sliding move" and the other two "bumping moves". The arrow on the left indicates the vertical direction.

asymmetry of the branching after the move, we say that the upper-right region "slides over" the upper-left region and creates the disc.

More in general, each instance of branched move can be viewed as a local sliding of a region over some neighboring one: in Figures 5 and 6 the sliding region is always the one which, after the application of the move, is the uppermost with respect to the depicted vertical direction. We warn the reader that, in the following section, with an abuse of notation, we will often call the small disc created by a positive branched move with the same name as the region over which the sliding has been performed; anyhow, this abuse will always be explicitly pointed out.

It has already been proved in [5][Chapter 3] that any lune and  $2 \neq 3$ -move is branchable, but that there are some inverse lune-moves and  $2 \neq 3$ -moves which are not branchable. Let us now analyze the branched versions of the bubble move, referring to Figure 3 for the notation.

If one assigns an orientation to  $D$  such that the orientation it induces on  $c$  is the same as the one induced by  $D^0$  on  $c$ , then the bubble move is said to be a sliding bubble move. The other case is called bumping bubble move; as shown in Figure 7, while performing an embedded bumping bubble move inside an oriented 3-manifold, two subversions of the move can be distinguished depending on whether  $D$  lies "over" or "under"  $D^0$ ; indeed the orientation of  $D^0$  and the orientation of the ambient manifold allow us to distinguish an upper and a lower face of  $D^0$ .

In [5], Benedetti and Petronio proved that every orientable 3-manifold admits a branched spine. Moreover, in [5] and [7] they identified a refined topological structure which is naturally encoded by a branching on a spine. Indeed, the vertical vector field in Figure 4 determines a well-defined homotopy class of vector fields on the ambient manifold which are positively transverse to the spine, whose orbits are properly embedded arcs and which are transverse to the boundary of the manifold except in a finite set of simple closed curves where they are tangent in a concave fashion. These particular kinds of vector fields were called "Concave Transversing Fields" by Benedetti and Petronio who, in [5] and [7] among a series of other results, proved a calculus for manifolds equipped with these fields, which we very roughly summarize as follows:

**Theorem 2.6.** To each embedded branched spine one can naturally associate an homotopy class of Concave Transversing Fields; moreover, any two branched spines encoding the same class, are connected by a sequence of embedded branched moves of the types which in Figures 5, 6 and 7 are called "sliding"-moves. If the ambient manifold is closed then the sequence can be chosen to contain no bubble move.

The above result represents a highly refined calculus for branched spines and was used in [6] as a fundamental step to produce topological invariants of homotopy classes of Concave Transversing Fields.

### 3. A calculus for branched spines of 3-manifolds

If one is interested in representing 3-manifolds by means of branched spines but is not interested in the particularly refined structure that the branching encodes, then one needs to find a calculus for branched spines allowing one to apply moves which change the homotopy class of Concave Transversing Fields represented by the spines to include all of them. We then prove the following:

**Theorem 3.1.** Let  $M$  (with  $\partial M$  possibly empty) be an oriented and compact 3-manifold and let  $P_1$  and  $P_2$  be two branched standard spines of  $M$ . There exists a sequence of branched moves including 2 ! 3-moves, lune-moves and bubble-moves connecting  $P_1$  and  $P_2$ . Moreover, the sequence can be constructed so that at any step the spines involved are standard.

**Proof of 3.1.** By the calculus of Matveev-Piergallini, any two standard spines of  $M$  are connected by a sequence of 2 ! 3-moves. Moreover, by a result of Y. Makovetsky (see [10]), it is possible to choose two sequences of positive 2 ! 3-moves connecting respectively  $P_1$  and  $P_2$  to the same standard spine  $P$  of  $M$ . Since these sequences are composed by positive moves, they are branchable and hence they connect  $P_1$  and  $P_2$  to two different branched versions of the same spine  $P$ . Let us call these two branchings on  $P$  respectively  $b_1$  and  $b_2$ . In what follows, we will show that, using also branched versions of bubble-moves, lune and 2 ! 3-moves, it is possible to connect the branched spine  $(P; b_1)$  to  $(P; b_2)$ .

Let  $R_1^+; \dots; R_n^+$  be the regions of  $P$  oriented according to  $b_1$ ; since  $M$  is oriented, it makes sense to speak of the upper face and of the lower face of a region of  $P$  with respect to a branching. Apply a bumping bubble-move as shown in the central part of Figure 7 to each region  $R_i^+$  over which  $b_1$  and  $b_2$  differ, so that the bubbles are attached along the upper face of the region with respect to  $b_1$  and call  $R_i$  the new discs attached by the bubble-moves ( $\mathbb{D}$  in Figure 7). With an abuse of notation, exploiting the asymmetry of the bumping bubble-moves, we will call  $R_i^+$  also the small disc ( $\mathbb{D}^0$  in Figure 7) created inside  $R_i^+$  by the gluing of  $R_i$ . Note that the polyhedron  $P_1^0$  obtained after the application of these moves contains  $(P; b_1)$  as a branched sub-polyhedron and in particular for each edge or vertex of  $P$  there is a corresponding one in  $P_1^0$ ; moreover,  $P_1^0$  is necessarily non standard: we will sketch how to restore the standard setting in the end of the section. Analogously, let us call  $P_2^0$  the polyhedron obtained by applying the above procedure using the branching  $b_2$  to choose the upper faces of the regions. It is clear that  $P_1^0$  and  $P_2^0$  are branched version of the same polyhedron  $P^0$ ; we keep calling  $b_1$  and  $b_2$  their branchings.

The idea of the proof is to slide the regions  $R_i$  in  $P_1^0$  to a final position where the roles of  $R_i^+$  and of  $R_i$  are exchanged and so, in particular, each  $R_i^+$  appears as a bubble applied to the center of  $R_i$ , on its upper face: this connects  $P_1^0$  and  $P_2^0$  by a sequence of branched moves (not including bubble-moves).

Here and in what follows we will use the natural identification induced by a branched move between the regions of a polyhedron before and after the move as explained in the preceding section. Moreover, for the sake of simplicity, we suppose that the edges and the vertices we deal with are touched by distinct regions; this is not true in general but the proof can be easily adapted to the general case using local names for the regions

around the edges and the vertices instead of the names  $R$ . We split the proof in two steps:

- (1) For each edge  $e$  of  $P$  we use positive bump moves near the corresponding edge  $f$  in  $P_1^0$  to create an edge such that if  $e$  is touched by  $R_i^+, R_j^+$  and  $R_k^+$  in  $P$  then the new edge is touched by  $F(R_i^+), F(R_j^+)$  and  $F(R_k^+)$ , where  $F(R^+) = R^+$  if  $b_1$  equals  $b_2$  on  $R^+$  in  $P$  and is  $R^-$  otherwise. This sequence of moves modifies  $P_1^0$  creating some additional singular locus and hence producing a polyhedron no longer homotopic to  $P^0$ , but since it acts only near the center of the edges of  $P_1^0$ , the vertices of  $P_1^0$  and hence of  $P$  are identified with a subset of the vertices of the resulting polyhedron.
- (2) For each vertex  $v$  of  $P$ , we apply a sequence of branched moves to the corresponding vertex  $w$  in the polyhedron obtained after Step 1 to create a vertex such that if  $R_i^+, R_j^+, R_k^+, R_l^+, R_m^+$  and  $R_n^+$  are the regions of  $P_1^0$  touching  $v$  then the vertex is touched by the regions  $F(R_i^+), F(R_j^+), F(R_k^+), F(R_l^+), F(R_m^+)$  and  $F(R_n^+)$  (where, again,  $F(R^+) = R^+$  if  $b_1$  and  $b_2$  are equal in  $P$  on  $R^+$  and is  $R^-$  otherwise). The sequence of moves we apply has also the effect of eliminating the extra singular locus created during the first step so that the final polyhedron we get is  $P_2^0$ .

Step 1. First of all, note that there are exactly 6 possible different branchings on the neighborhood of an edge of a spine (of the 8 possible 3-uples of orientations on the regions touching the edge, two are to be excluded since of the branching condition). Moreover, each branching on an edge together with the orientation of  $M$ , produces a cyclic ordering of the regions touching it and a notion of up and down near it, so that we can define as shown in Figure 8 the regions of type 1, 2 and 3 with respect to the branching on the edge.

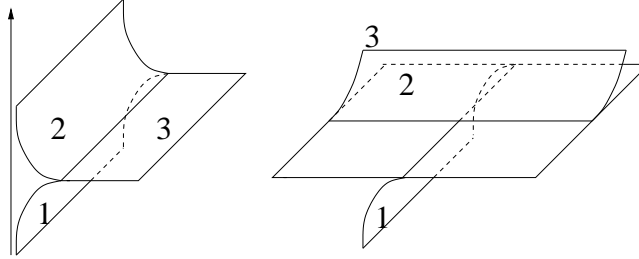


Figure 8. In this picture we show how to determine the regions of type  $i = 1; 2; 3$  near an edge and near a vertex. In the picture we use the right-hand rule and vertical direction drawn on the left to determine the orientations of the regions.

Let  $e$  be an edge of  $P$  where  $b_1$  and  $b_2$  are different,  $f$  the corresponding edge in  $P_1^0$  and let respectively  $R_i^+, R_j^+$  and  $R_k^+$  be the regions of type 1, 2 and 3 with respect to the branching  $b_1$  on  $e$ .

Suppose that  $R_i^+$  is the only region touching  $e$  on which  $b_1$  and  $b_2$  differ; we will now exhibit a sequence of 2 positive bumping lune-moves near  $f$  in  $P_1^0$  which creates an edge touched by  $R_i^+, R_j^+$  and  $R_k^+$  and some additional singular locus which will be eliminated in Step 2.

Since  $R_i^+$  is oriented in the opposite way by  $b_1$  and  $b_2$ , to get  $P_1^0$  from  $P_1$  we applied a bumping bubble-move over this region and created a disc  $R_i^-$  on the upper (with respect



to  $b_1$ ) face of it. Apply a bumping lune-move to slide  $R_i^-$  over a little disc contained in  $R_j^+$  as shown in the upper part of Figure 9. This splits  $f$  adding two new vertices and creates a new small disc and a new singular edge  $f^0$  touched by  $R_i^-$ ,  $R_j^+$  and the disc itself. Apply now another bumping lune-move to slide  $R_i^+$  over  $R_i^-$  passing through the disc as shown in the lower-left part of Figure 9. The edge  $f^0$  is split by two new vertices and a new small disc is created. With an abuse of notation we will call this new small disc  $R_i^-$ ; indeed it can be viewed as a smooth continuation of  $R_i^-$  over the edge separating them. After this move, the small straight edge connecting the two vertices in the lower-right part of Figure 9 is touched by the regions  $R_i^-$ ,  $R_j^+$  and  $R_k^+$ : we obtained the singular edge we were searching for. The side-effect of the sequence of moves just described is to create two pairs of new vertices positioned symmetrically with respect to the center of the edge: we will show in Step 2 how to eliminate these vertices.

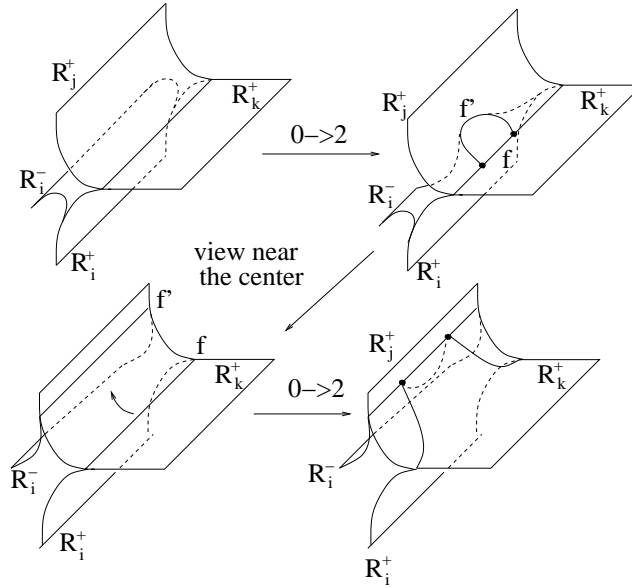


Figure 9. In this picture we show the sequence of moves used to exchange near the center of an edge of  $P_1^0$  a region  $R_i^+$  of type 1 with respect to  $b_1$  with its companion  $R_i^-$ . The first move is a bumping lune-move shifting  $R_i^-$  over  $R_i^+$ ; then we concentrate on the central part of the picture and we apply another bumping lune-move to slide  $R_i^+$  over  $R_i^-$ .

Suppose now that  $b_1$  and  $b_2$  differ only on  $R_j$ . We will now exhibit a sequence of 2 sliding lune-moves near  $f$  in  $P_1^0$  creating a new edge  $f^0$  touched by  $R_i^+$ ,  $R_j^+$  and  $R_k^+$ . Apply a sliding lune-move to push  $R_j$  onto a little disc contained in  $R_k^+$  and containing the center of  $f$  in its boundary. The boundary of the little disc is formed by  $f$  and another small singular edge  $f^0$  (see the upper part of Figure 10). Then, we apply another sliding lune-move to push  $R_j^+$  over  $R_j^-$  near the center  $f^0$  passing over the small disc. This creates another small disc "contained" in  $R_j^-$  which, with an abuse of notation, we will call  $R_j^-$ . The sequence creates the edge touched by  $R_i^+$ ,  $R_j^-$  and  $R_k^+$  we were

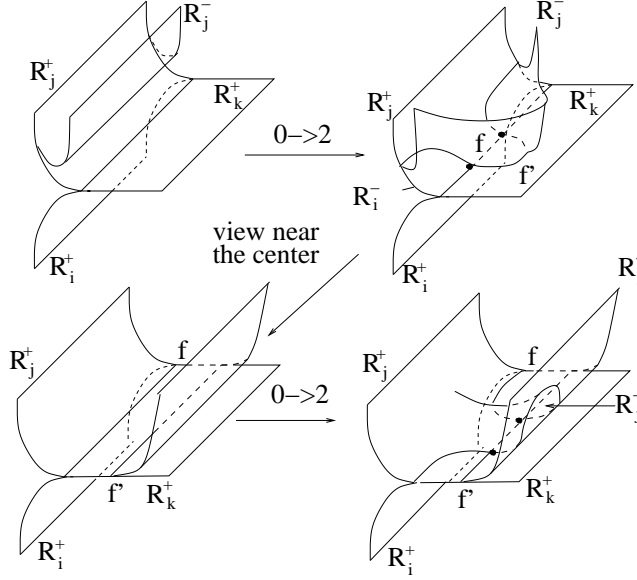


Figure 10. In this picture we show how to revert the orientation of a region of type 2 near the center of an edge. In the first step we apply a sliding lune-m ove to push  $R_i^+$  over  $R_i^-$ , then we concentrate on the center part of the picture and we apply another sliding lune-m ove to push  $R_i^+$  over  $R_i^-$ .

searching for. Again, as a side-effect of the sequence, two pairs of new vertices disposed symmetrically with respect to the edge appear.

Let us now show how to conclude Step 1 in the general case around  $e$ . Starting from  $f$ , we want to produce an edge in  $P_1^0$  touched by the regions  $F(R^+)$  (where  $F(R^+) = R^+ \cap b_1$  and  $b_2$  do not differ on  $R^+$ ). To do this, we "substitute" the regions one by one using the above sequences of moves. Consider the following algorithm:

- (1) Let  $X$  be the region of type 1 with respect to the branching on  $f$ . If  $X = F(R^+)$  for some  $R^+ \in P_1^0$ , go to 2, otherwise apply the sequence of Figure 9 to  $f$ : this produces a new branched edge which we keep calling  $f$  whose regions are still indicized by the three-uple  $f_i; j; k_g$  and in which one more region is of the form  $R = F(R^+)$ . Go to 2.
- (2) Let  $Y$  be the region of type 2 with respect to the branching on  $f$ . If  $Y = F(R^+)$  for some  $R^+ \in P_1^0$  stop, otherwise apply the sequence of Figure 10 to  $f$ : this produces a new branched edge which we keep calling  $f$  whose regions are still indicized by the three-uple  $f_i; j; k_g$  and in which one more region is of the form  $R = F(R^+)$ ; go back to 1.

Since the regions around  $f$  are indicized in  $f_i; j; k_g$ , we can "pullback" on  $e$  the branching of  $f$  and call it  $b(f)$ . To compare  $b(f)$  and  $b_1$  on  $e$  we stipulate that they differ on a region  $R_x^+$  touching  $e$  if the corresponding region touching  $f$  is  $R_x^+$ . Consequently,  $b(f)$  and  $b_2$  differ on a region  $R_x^+$  near  $e$  if the corresponding region touching  $f$  is  $R_x^+$  and  $b_1$  and  $b_2$  differ on  $R_x^+$ .

We claim that when the above algorithm stops  $b(f) = b_2$  on  $e$ . Indeed they cannot differ on a region of type 1 or 2 near  $e$  with respect to  $b(f)$  since otherwise the algorithm

would not have stopped. But then, they cannot differ on the remaining region since otherwise  $b_2$  would not satisfy the branching condition on  $e$  (by construction  $b(w)$  does).

Roughly speaking, by applying the above procedure to  $P_1^0$  for each edge of  $P$ , one obtains a new branched spine which, near the centers of some edges is branched according to  $b_2$ , near the vertices corresponding to those of  $P$  is still branched according to  $b_1$  and which contains some additional singular locus which will delete in the next Step.

Step 2. Let  $w$  be a vertex of the branched polyhedron obtained after Step 1 and corresponding to a vertex  $v$  of  $P$ . A branching canonically equips each edge of a spine with an orientation (the one induced by two of the 3 regions touching the edge) and this allows us to identify 3 particular regions around each branched vertex. These regions are those which, in the neighborhood of the vertex, orient both the edges in their boundary positively, and are shown in Figure 8. We call them regions of type 1, 2 and 3; we tell regions of type 1 from those of type 3 by means of the orientation of  $M$ : the type 1 is the lower one with respect to the positively oriented normal to the spine in the vertex.

Suppose by now that  $b_1$  and  $b_2$  differ near  $v$  only on the region  $R_i^+$  of type 1 w.r.t  $b_1$  and let us exhibit the sequence concluding Step 2 on  $v$  in this case.

Let  $e_1$  and  $e_2$  be the two edges of  $P$  touching  $v$  and contained in the boundary of  $R_i^+$ . Note that  $R_i^+$  is of type 1 w.r.t  $b_1$  also for  $e_1$  and  $e_2$  (see Step 1) and hence during Step 1 we applied the sequence of moves of Figure 9 to the edges  $f_1$  and  $f_2$  in  $P_1^0$  corresponding to  $e_1$  and  $e_2$ . In particular, the first moves applied on these two edges during Step 1 are bumping lune-moves shifting  $R_i$  over small discs contained in the regions of type 2 respectively for  $f_1$  and for  $f_2$  and which, near  $w$  appear as horizontal. Then near  $w$  we see the pattern described in the upper-left part of Figure 11. Apply an inverse bumping  $2!3$ -move and complete the shifting of  $R_i$  near  $w$  (see the upper-right part of Figure 11). Then, applying a bumping  $2!3$ -move we slide  $R_i^+$  over a small disc on  $R_i$  which, with an abuse of notation, we will call  $R_i$ . Finally, since the last moves of the sequence of Figure 9 applied in Step 1 are two bumping lune-moves near  $f_1$  and  $f_2$  sliding  $R_i^+$  over  $R_i$ , we are in the situation depicted in the lower-left part of the same figure. We can then apply two inverse bumping lune-moves to eliminate the two small discs horizontal in the lower-left part of the figure and slide the region  $R_i^+$  over  $R_i$  as shown in the lower-right part of the figure. That way, the vertices which had been created during Step 1 on the edges  $f_1$  and  $f_2$  disappear and we created a new vertex touched by the same regions as  $v$  with the only exception of  $R_i^+$  which has been substituted by  $R_i$ . This concludes Step 2 in this case.

Let us now suppose that  $b_1$  and  $b_2$  differ near  $v$  only in the region of type 2 w.r.t  $b_1$  and let  $R_j^+$  be this region.

Let again  $e_1$  and  $e_2$  be the two edges of  $P$  in the boundary of  $R_j^+$  touching  $v$  and  $f_1$  and  $f_2$  the corresponding edges in  $P_1^0$ . Note that, w.r.t  $b_1$ ,  $R_j^+$  is of type 1 for one of the two edges (say  $e_1$ ) and of type 2 for the other one ( $e_2$ ). Moreover, note that the region near  $v$  which is of type 1 for  $e_2$  is also of type 1 for  $v$ , hence, by hypothesis, this region in  $P$  is oriented the same way by  $b_1$  and  $b_2$ . Then the moves applied on  $f_1$  during Step 1 are those of the sequence of Figure 9: in particular the first one is a bumping lune-move sliding the region  $R_j$  over the center of the edge. On  $f_2$ , the moves of Step 1 are those of the sequence of Figure 10 and the first one is a sliding lune-move pushing  $R_j$  near the center of the edge over a small disc contained in the region of type 3 for  $f_2$ . Hence, near  $w$ , the polyhedron after Step 1 appears as shown in the upper-left square of Figure 12.

By applying an inverse sliding  $2!3$ -move, one shifts  $R_j$  over  $w$  as shown in the upper-left part of the figure. Finally, since the last moves of the sequences applied

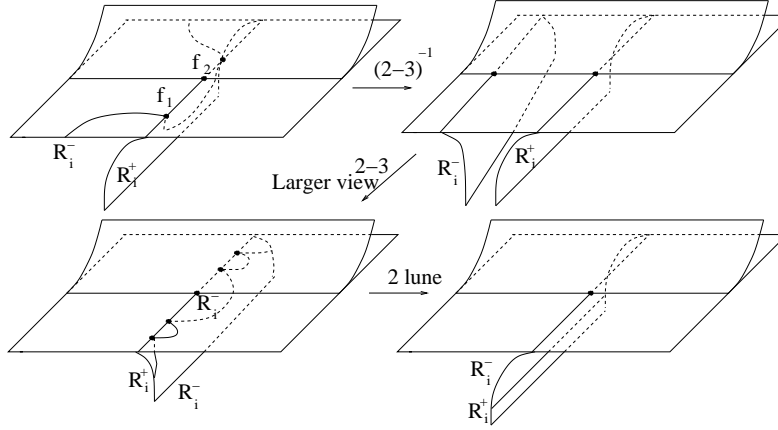


Figure 11. In this picture we show the sequence used in the case when the branchings on a vertex differ on a region of type 1 with respect to the first branching.

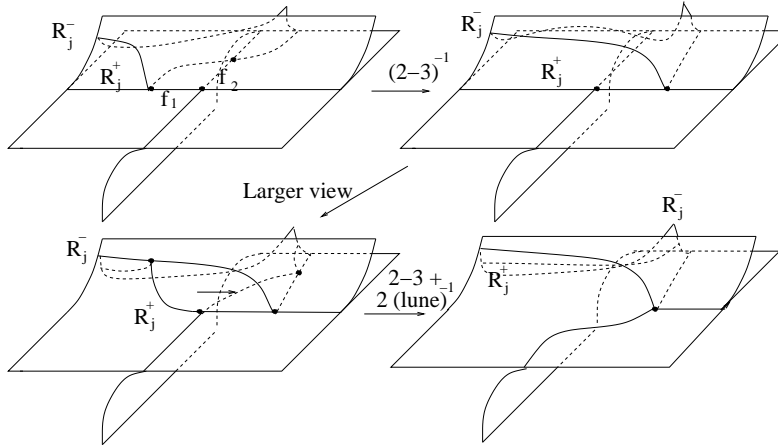


Figure 12. In this picture we show the sequence used in the case when the branchings on a vertex differ on a region of type 2 with respect to the first branching. Note that, for the sake of clarity, in the above picture we do not draw some regions and we limit ourselves to outline their boundary curves.

during Step 1 on the edges  $f_1$  and  $f_2$  slid  $R_j^+$  over  $R_j^-$  we are left in the case shown in the lower-left part of the figure. Then we apply a  $2 \rightarrow 3$ -move to slide  $R_j^+$  over a small disc contained in  $R_j^-$  as indicated by the small arrow in the lower-left part of the figure; with an abuse of notation we call this disc  $R_j^-$ . Then we perform two inverse lune-moves to eliminate the two small discs visible in the lower-left part of the figure and complete the sliding of  $R_j^+$  over  $R_j^-$ . This completes Step 2 in this case.

Until now we showed how to conclude Step 2 when  $b_1$  and  $b_2$  differ on a region of type 1 or 2 near  $v$ . Now we examine the case when  $b_1$  and  $b_2$  differ only on the region  $R_k^+$  of type 3 w.r.t  $b_1$  near  $v$ .

Let again  $e_1$  and  $e_2$  be the two edges in the boundary of  $R_k^+$  and  $f_1$  and  $f_2$  the corresponding edges in  $P_1^0$ , so that  $e_2$  is also in the boundary of the region which is of type 2 with respect to  $b_1$  on  $v$ . Note that  $R_k^+$  is of type 2 for both the edges w.r.t.  $b_1$ . Moreover, by hypothesis, the regions of type 1 and 2 w.r.t.  $b_1$  near  $v$  are oriented the same way by  $b_1$  and  $b_2$ , this implies that also the region near  $v$  which contains in its boundary  $e_1$  and orients it in the same way as  $R_k^+$  is oriented the same way by  $b_1$  and  $b_2$  (otherwise  $b_2$  would not define a branching). Hence, during Step 1 we applied both on  $f_1$  and on  $f_2$  the sequence of moves of Figure 10. Then, near  $w$ , we are in the situation depicted in the upper-left part of Figure 13. We apply an inverse sliding  $2 \rightarrow 3$ -move near  $w$  to slide  $R_k$  over the horizontal plane (see the upper-right part of the figure). Then we apply a sliding  $2 \rightarrow 3$ -move to slide  $R_k^+$  over a small disc contained  $R_k$  near the vertex. With an abuse of notation we will call this disc  $R_k$ . Since in the sequence of moves applied during Step 1 over each edge a sliding lune-move has been performed to slide  $R_k^+$  over  $R_k$ , we are now in the situation depicted in the lower-left square of the figure. To finish, we then apply two inverse sliding lune-moves to slide  $R_k^+$  over  $R_k$  and eliminate the two small discs present in the lower left part of the figure.

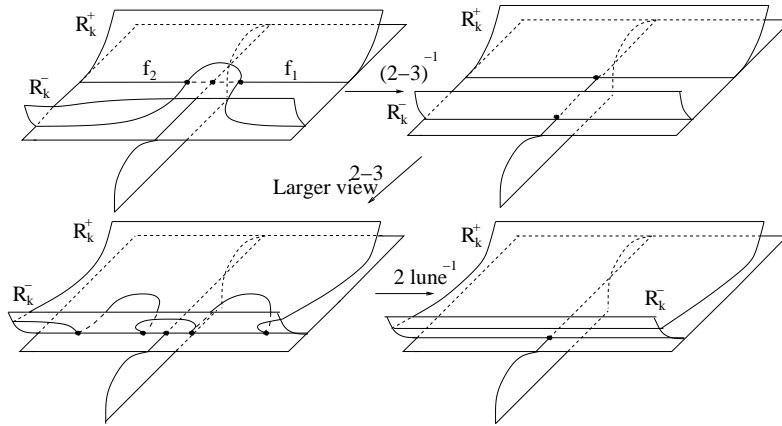


Figure 13. In this picture we show the sequence used in the case when the branchings on a vertex differ on a region of type 3.

We now claim that the sequences shown in Figures 11, 12 and 13 are sufficient to complete Step 2 in the general case when  $b_1$  and  $b_2$  differ on more than one region near  $v$ .

Now let  $R_i^+, R_j^+, R_k^+, R_l^+, R_m^+$  and  $R_n^+$  be the regions of  $P$  around  $v$ . In the vertex  $w$  of the polyhedron obtained after Step 1 and corresponding to  $v$ , we want to "substitute" each region  $R^+$  with  $F(R^+)$  (where  $F(R^+) = R^+ \cup b_2$  and  $b_2$  do not differ on  $R^+$ ), that is apply suitable sequence of moves which produce a new vertex touched by the six regions  $F(R^+)$ . To do this we substitute the regions one by one using the sequences exhibited above. Consider the following algorithm :

- (1) Let  $X$  be the region of type 1 with respect to the branching on  $w$ . If  $X = F(R^+)$  go to 2, otherwise apply the sequence of Figure 11 to  $w$ : this produces a new branched vertex which we keep calling  $w$  whose regions are still indicized by the six-uple  $f_i; j; k; l; m; n$  and in which one more region is of the form  $R^-$ . Go to 2.

- (2) Let  $Y$  be the region of type 2 with respect to the branching on  $w$ . If  $Y = F(R^+)$  go to 3 otherwise apply the sequence of Figure 12 to  $w$ : this produces a new branched vertex which we keep calling  $w$  whose regions are still indicized by the six-uple  $fi; j; k; l; m; ng$  and in which one more region is of the form  $R^-$ ; go back to 1.
- (3) Let  $Z$  be the region of type 1 with respect to the branching on  $w$ . If  $Z = F(R^+)$  stop otherwise apply the sequence of Figure 13 to  $w$ : this produces a new branched vertex which we keep calling  $w$  whose regions are still indicized by the six-uple  $fi; j; k; l; m; ng$  and in which one more region is of the form  $R^-$ . End.

Since  $w$  is branched and the regions touching it are indexed in  $fi; j; k; l; m; ng$ , we can "pullback" on  $v$  the branching on  $w$  which we will call  $b(w)$  and compare it with  $b_1$  and  $b_2$ :  $b(w)$  differs from  $b_1$  on a region  $R_x^+$  if and only if  $w$  is touched by  $R_x^-$ . Analogously  $b(w)$  and  $b_2$  differ on a region  $R_x^+$  if  $b_1$  and  $b_2$  differ on it and  $w$  is touched by the region  $R_x^-$ .

We claim that, when the algorithm stops, the regions of the form  $R^-$  touching  $w$  are exactly those over which  $b_1$  and  $b_2$  differ and then  $b_2 = b(w)$  near  $v$ . Indeed, the above algorithm stops when the regions of type 1, 2 and 3 around  $w$  are all of the form  $F(R^-)$ ; clearly, this is achieved in at most 6 steps. Then, in particular,  $b_2$  and  $b(w)$  define branchings coinciding on the regions of type 1, 2 and 3 w.r.t.  $b(w)$ . This implies that  $b_2$  and  $b(w)$  are equal on all the regions since if  $b_2$  differed from  $b(w)$  on another region then the branching condition would not be satisfied by  $b_2$ . It is important to note that the algorithm above can be followed until its end since during Step 1 we used an algorithm based on the edges of  $P$  producing exactly the extra vertices eliminated by the sequences of Figures 11, 12 and 13 and ordered compatibly. This concludes Step 2.

Now let us note that after Step 2, the polyhedron one obtains is homeomorphic to  $P^0$  (during Step 2 we eliminated all the extra structures constructed during Step 1), and its branching coincides with the one given by  $b_2$  since, using embedded branched moves, we exchanged the roles of the regions  $R^+$  with those of the regions  $R^-$  having the opposite orientation. We are now left to prove that the sequence of moves we used can be improved to a sequence passing only through standard polyhedra: we limit ourselves to sketch the idea of the proof. For each region  $R_i^+$  in  $P$  let us choose an edge  $e_i \in \text{Sing}(P)$  touched by  $R_i^+$ . Then at the beginning of the proof, if  $b_1(R_i^+) \neq b_2(R_i^+)$ , instead of applying a bubble move inside  $R_i^+$  we apply a standard bubble move (whose non branched version is shown in the right part of Figure 3) gluing  $R_i^-$  along  $e_i$  slightly aside from the center of the edge and on the upper side of  $R_i^+$  (with respect to  $b_1$ ). The curve  $\partial R_i^-$  will bound a disc in  $P$  formed by the union of two discs, one "contained" in  $R_i^+$  and the other, call it  $D_i$  coming from another region touching  $e_i$ . Now apply Step 1 and then apply an inverse lune move to slide  $R_i^-$  out of  $D_i$ . It can be checked that the polyhedron one obtains is equal to the result of Step 1 obtained by following the proof in the non standard case, but never passes through non standard polyhedra so that one can proceed with Step 2. To ensure that also during Step 2 one does not produce non standard polyhedra, it is sufficient to observe that the only moment when such a polyhedron can be obtained is when one concludes one of the sequences of Figures 11, 12 and 13 through the pair of inverse lune moves and the region to be slid, after the move, becomes a bubble over another region of the polyhedron. In this case it is sufficient to perform just one of the two inverse lunes and proceed with Step 2 (which will no more involve that region).

3.1

## References

1. Baseilhac, S. and Benedetti, R., \QHI, 3-manifolds scissors congruence classes and the volume conjecture", *Geom. Topol. Monogr. Invariants of knots and 3-manifolds* 4 (2001), 13-28.
2. Baseilhac, S. and Benedetti, R., \QHI Theory II, Dilogarithmic and Quantum Hyperbolic Invariants of 3-Manifolds with  $PSL(2;C)$ -Characters", [xxx.arxiv.org/math.GT/0211061](http://xxx.arxiv.org/math.GT/0211061) (2002).
3. Baseilhac, S. and Benedetti, R., \Quantum Hyperbolic Invariants of 3-Manifolds with  $PSL(2,C)$ -Characters", [xxx.arxiv.org/math.GT/0306280](http://xxx.arxiv.org/math.GT/0306280) (2003).
4. Baseilhac, S. and Benedetti, R., \Classical And Quantum Dilogarithmic Invariants of Flat  $PSL(2,C)$ -Bundles Over 3-Manifolds", [xxx.arxiv.org/math.GT/0306283](http://xxx.arxiv.org/math.GT/0306283) (2003).
5. R. Benedetti, C. Petronio, \Branched Standard Spines of 3-manifolds", *Lecture Notes in Math.*, vol. 1653, Springer-Verlag, Berlin-Heidelberg-New York, 1997.
6. R. Benedetti, C. Petronio, \Reidemeister-Turaev torsion of 3-dimensional Euler structures with simple boundary tangency and pseudo-legendrian knots", *Manuscripta Mathematica* 106 (2002) 1, 13-61.
7. R. Benedetti, C. Petronio, \Combed 3-manifolds with concave boundary, framed links, and pseudo-Legendrian links", *J. Knot Theory Ramifications* 10 (2001) 1, 1-35.
8. J.L. Dupont, C-H. Sah, \Scissors congruences II", *J. Pure and App. Algebra* 44 (1987), 137-164.
9. S.M. Atveev, \Transformations of special spines and the Zeeman conjecture", *Math. USSR Izvestia* 31 (1988), 423-434.
10. A.Yu. Makovetski, A.Yu., \Transformations of special spines and special polyhedra", *Math. Notes* 65 (1999), 295-301.
11. R. Piergallini, \Standard moves for standard polyhedra and spines", *Rend. Circ. Mat. Palermo* 37 (1988), suppl. 18, 391-414.
12. V. Turaev, O.Viro, \State sum invariants of 3-manifolds and 6j-symbols", *Topology* 31 (1992), 865-904.

Scuola Normale Superiore

Piazza dei Cavalieri 7, 56127 Pisa, Italy

f.costantino@sns.it

Scuola Normale Superiore, Piazza dei Cavalieri 7, 56126 Pisa, Italy

E-mail address: f.costantino@sns.it